Proceedings Paper:

Hoang, K. orcid.org/0000-0001-7463-9681, Lazari, P. and Atallah, K. (2021) Analysis and control development of IPM traction machines with skewed rotor using unskewed machine model. In: Proceedings of IECON 2021 – 47th Annual Conference of the IEEE Industrial Electronics Society. 47th Annual Conference of the IEEE Industrial Electronics Society (IECON2021), 13-16 Oct 2021, Virtual Conference (Toronto, ON, Canada). Institute of Electrical and Electronics Engineers . ISBN 9781665402569

https://doi.org/10.1109/IECON48115.2021.9589991

Analysis and Control Development of IPM Traction Machines with Skewed Rotor using Unskewed Machine Model

Khoa Dang Hoang
Dept. of Electronic and Electrical Engineering
The University of Sheffield
Sheffield, United Kingdom
k.hoang@sheffield.ac.uk

Panagiostic Lazari
Dept. of Multidisciplinary Engineering Education
The University of Sheffield
Sheffield, United Kingdom
p.lazari@sheffield.ac.uk

Kais Atallah
Dept. of Electronic and Electrical Engineering
The University of Sheffield
Sheffield, United Kingdom
k.atallah@sheffield.ac.uk

***Abstract*—The paper presents a simplified analysis and control development method for IPM traction machines with skewed rotor using unskewed machine model. It is shown that the skewed machine characteristics under a given set of *dq*-axis currents could be obtained from the unskewed machine model using relevant modified *dq*-axis currents associated with the skewed information. Therefore, under the proposed method, the tested IPM machine model with skewed rotor could be rapidly derived from the unskewed machine model without FEA implementation for each skewed slice. It is demonstrated that in comparison with the FEA-based model, the proposed method could maintain up to 0.2% difference for both stator flux linkage and torque maps over *dq*-axis currents applied as well as 0.1% efficiency difference map over main torque speed operation. The proposed method is validated by FEA and measurement from a high-speed high-power (8000rpm, 80kW) IPM traction machine with skewed rotor.**

Keywords— Control development, IPM traction machine, multi-slices, skewed machine model.

I. INTRODUCTION

IPM machines are often selected for traction applications due to their rotor geometries resulting in high-torque and high-speed operation capability [1], [2]. However, IPM machine rotor geometries may also result in the machine high torque harmonic characteristics [2]. To reduce torque harmonics, optimum skewed technique with multi-rotor slices is often employed [3]. Basically, the optimum skewed angle is carefully selected to minimize high order torque harmonics (i.e. 6^{th} and 12^{th} components…) while maintaining maximum DC torque achievement. In practice, for machine analysis and control development, IPM machine model with skewed rotor under multi-slice technique is often obtained via superposition theorem of FEA result on each slice [3], [4]. Therefore, the higher number of skewed rotor-slices, the higher computational FEA is required.

To avoid high computational FEA, analysis methods for estimating the skewed machine characteristics from unskewed machine model were proposed in [5]-[7]. Influences of skewing on *dq*-axis inductances of PM machines were presented in [5] and [6] where skewed *dq*-axis inductances were computed from both unskewed *dq*-axis inductances using a skewed factor. However, only *dq*-axis inductances as a function of *q*-axis current were presented in [5]. On the other hand, since saturation level of IPM machines highly depends on *dq*-axis current applied [2], *dq*-axis inductance information of a skewed IPM machine obtained by applying a simple skewed factor to an unskewed IPM machine model as per shown in [5] and [6] may not be highly accurate under high *dq*-axis currents applied. A modified technique to predict *dq*-axis flux linkages over *dq*-axis currents applied was proposed in [7] where only static torque measurements were validated. It is noted that for IPM traction machine, machine efficiency map over torque speed operation is highly essential [1], [2].

The paper presents an analysis and control development method for IPM traction machines with multi-skewed rotor slices using unskewed machine characteristics. It is shown that analysis model of the tested IPM machine with skewed rotor could be rapidly derived from the unskewed machine model without FEA requirement for each skewed slice. It is demonstrated that in comparison with the FEA-based model, the proposed method could maintain up to 0.2% differences for stator flux linkage and torque maps as well as 0.1% efficiency difference map over main torque speed operation. The proposed method is validated by FEA and measurement on a high-speed high-power (8000rpm, 80kW) IPM traction machine with skewed rotor.

II. MODELING AND CONTROL DEVELOPMENT OF IPM TRACTION MACHINE WITH SKEWED ROTOR

A. Tested IPM Machine with Skewed Rotor

In Table I, specification of the tested machine is presented. The original unskewed design is depicted in Fig. 1(a) whereas the skewed designs of the tested machine are respectively presented in Figs. 1(b) and 1(c). In comparison with the unskewed design, Fig. 1(a), the tested IPM machine rotor is half-skewed backward [see Fig. 1(b)] and half-skewed forward [see Fig. 1(c)] to reduce machine torque harmonics. Torque and voltage waveform under FEA of the tested machine at 1000rpm under no-load condition and maximum peak torque condition (240Nm) are respectively presented in Figs. 2 and 3. As can be seen, due to the skewed technique, a significant reduction of torque ripples cold be achieved for the tested machine over its torque generation. Figs. 2 and 3 also demonstrates that for the tested machine with skewed rotor, FEA for each skewed slice should be implemented and then the skewed machine model could be obtained via superposition theorem considering all skewed rotor slices. It is noted that due to the equal active length for both the backward-skewed and forward-skewed slices, the unskewed *dq*-axis reference is also the skewed *dq*-axis reference under superposition theorem [see Fig. 2(b)].

B. Modelling and Control Development of Skewed Rotor IPM Traction Machines

Normally, the IPM machine model with skewed rotor for control development is often obtained by FEA. As aforementioned, for each specific skewed slice, a relevant FEA-based model is generated. Then, the combined model including all skewed slices are derived via superposition theorem. By way of example, Figs. 4 and 5 respectively presents torque and flux maps of the tested machine with half-skewed backward rotor and half-skewed forward rotor. As can be seen, under half-skewed backward model, a negative torque may obtain for the tested machine with zero q-axis current applied, Fig. 4(b). Also, under half-skewed forward rotor, a positive torque may obtain for the tested machine with zero q-axis current applied, Fig. 5(b). The torque and flux maps of the tested machine with skewed rotor under superposition theorem is depicted in Fig. 6. Obviously, the higher number of skewed slices, the higher computational FEA is required for obtaining the combined model.

TABLE I

SPECIFICATION OF TESTED IPM MACHINE

Peak torque (Nm)	240
Continuous torque (Nm)	75
Peak current (A)	460
Base speed (rpm)	2500
Maximum speed (rpm)	8000
DC-link voltage (V)	324
Number of pole pair	4

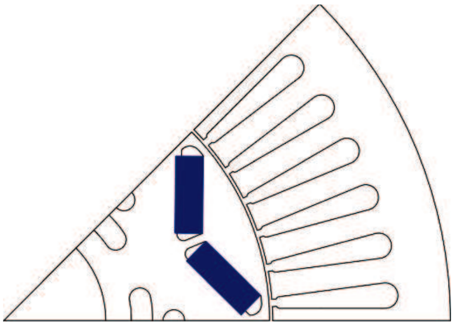

(a)

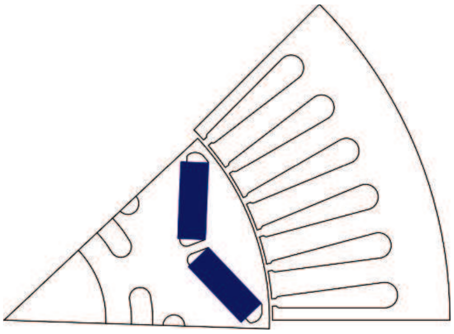

(b)

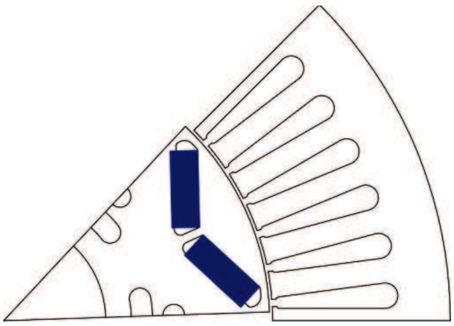

(c)

Fig. 1. Tested IPM machine geometries. (a) Unskewed structure. (b). Backward-skewed structure. (b). Forward-skewed structure.

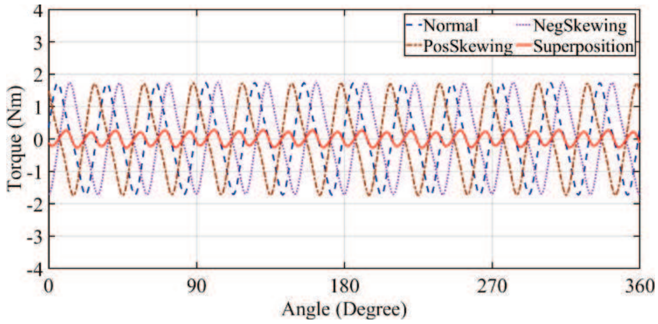

(a)

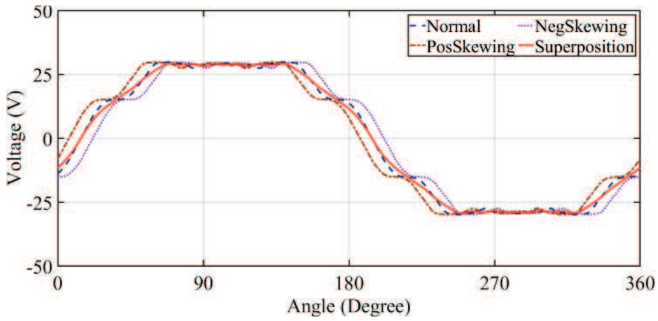

(b)

Fig. 2. Skewed effects on tested IPM machine under no-load condition, 1000rpm. (a) Torque waveform. (b) Back-EMF waveform.

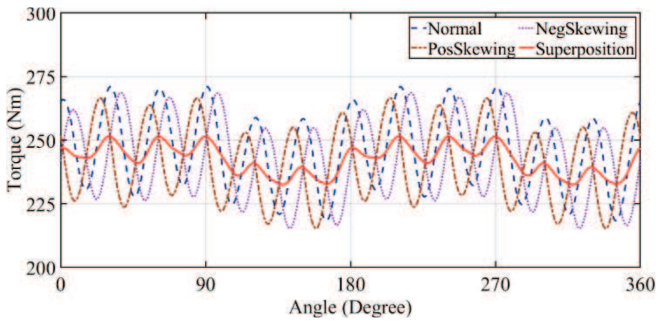

(a)

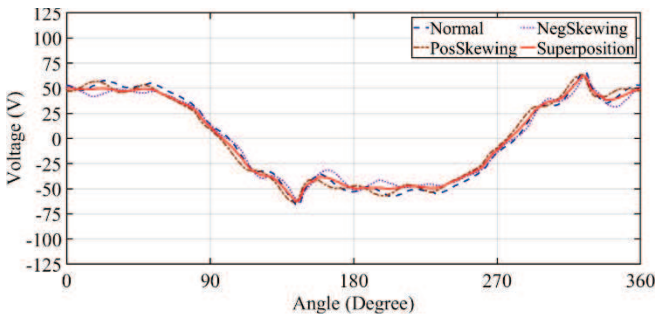

(b)

Fig. 3. Skewed effects on tested IPM machine under peak torque condition (240Nm), 1000rpm. (a) Torque waveform. (b) Voltage waveform.

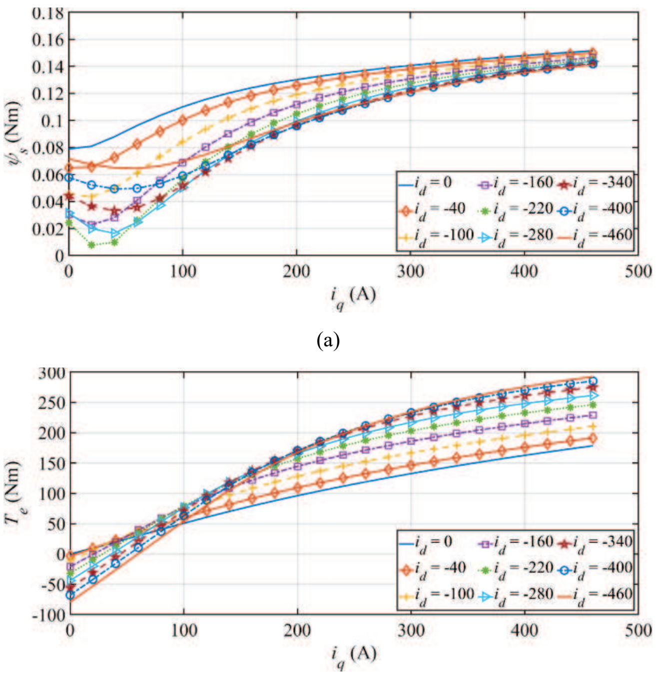

(a)

(b)

Fig. 4. Tested IPM machine characteristics with backward-skewed rotor, FEA model. (a) Stator flux linkage. (b) Torque.

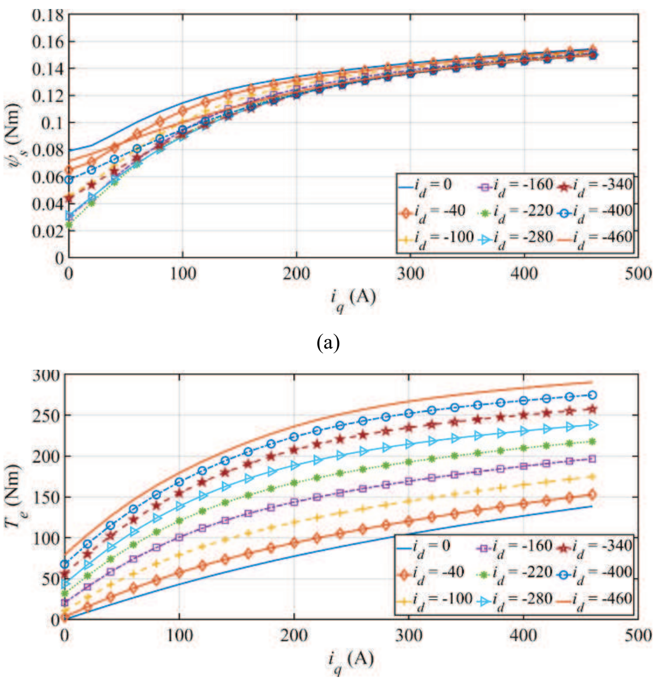

(a)

(b)

Fig. 5. Tested IPM machine characteristics with forward-skewed rotor, FEA model. (a) Stator flux linkage. (b) Torque.

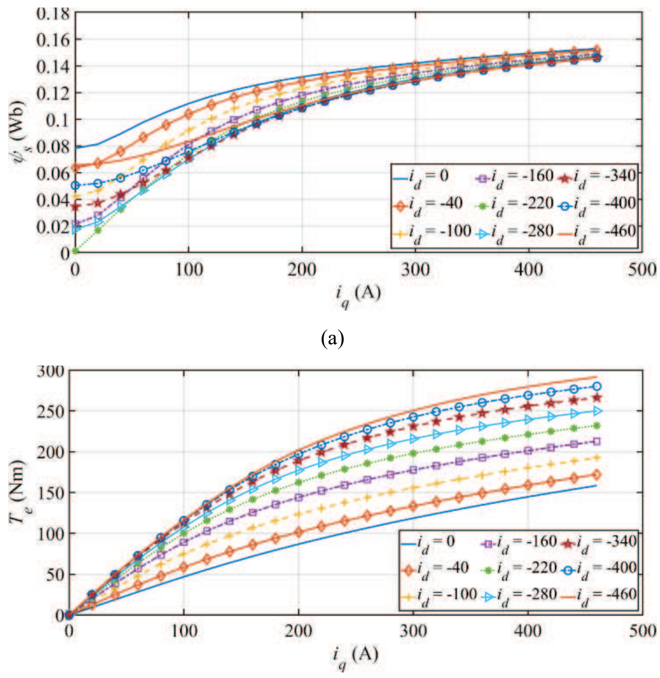

(a)

(b)

Fig. 6. Final tested IPM machine characteristics with multi-slice rotor under superposition theorem, FEA model. (a) Stator flux linkage. (b) Torque.

III. Proposed Analysis and Control Development of Skewed IPM Machine with Unskewed Model

A. Relation Between Dq-axis Currents under Skewed Rotor and Unskewed Rotor

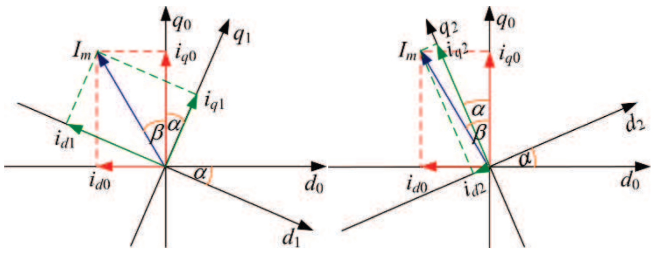

(a) (b)

Fig. 7. Relation between dq-axis current under unskewed structure and skewed structure. (a) Backward-skewed rotor. (b) Forward-skewed rotor.

The relation in dq-axis currents between the unskewed reference (d_0q_0-axis), the backward-skewed reference (d_1q_1-axis), and the forward-skewed reference (d_2q_2-axis) is respectively presented in Figs. 7(a) and 7(b). As can be seen, for a given set of dq-axis currents under the unskewed reference, relevant dq-axis currents seen by the backward-skewed reference and the forward-skewed reference could be computed by (1) to (4) where $i_{d0,q0}$ is the dq-axis current set in the unskewed reference; $i_{d1,q1}$ is the relevant dq-axis current set in the backward-skewed reference; $i_{d2,q2}$ is the relevant dq-axis current set in the forward-skewed reference. Using the obtained relevant dq-axis currents, stator flux linkage and torque maps under backward-/forward-skewed rotor in the relevant skewed references could be extracted from unskewed models as shown in (5) to (7) where $T_{e0,1,2}$ is respectively the machine torque under unskewed reference, backward-skewed reference, and forward-skewed reference; $\psi_{d0,1,2}$ is respectively the d-axis flux linkage under the unskewed reference, the backward-skewed reference, and the forward-skewed reference; $\psi_{q0,1,2}$ is respectively the q-axis flux linkage under the unskewed reference, the backward-skewed reference, and the forward-skewed reference.

$$i_{d1} = i_{d0}\cos(\alpha) - i_{q0}\sin(\alpha) \tag{1}$$

$$i_{q1} = i_{d0}\sin(\alpha) + i_{q0}\cos(\alpha) \tag{2}$$

$$i_{d2} = i_{d0}\cos(\alpha) + i_{q0}\sin(\alpha) \tag{3}$$

$$i_{q2} = -i_{d0}\sin(\alpha) + i_{q0}\cos(\alpha) \tag{4}$$

$$T_{e1,2}(i_{d0}, i_{q0}) = T_{e0}(i_{d1,2}, i_{q1,2}) \tag{5}$$

$$\psi_{d1,2}(i_{d0}, i_{q0}) = \psi_{d0}(i_{d1,2}, i_{q1,2}) \tag{6}$$

$$\psi_{q1,2}(i_{d0}, i_{q0}) = \psi_{q0}(i_{d1,2}, i_{q1,2}) \tag{7}$$

Since the control reference of the tested machine model under superposition theorem is similar to the unskewed reference (d_0q_0) [see Fig. 2(b)], dq-axis flux linkages under the skewed reference in (6) and (7) should be transferred into the unskewed reference using (8) to (11) where $\psi_{d,q1(0)}$ is the dq-axis flux linkages transferred from the backward-skewed reference into the unskewed reference; $\psi_{d,q2(0)}$ is the dq-axis flux linkages transferred from the forward-skewed reference into the unskewed reference. Under superposition theorem, the tested machine model for analysis and control development could be obtained by (12) to (14) where T_e is the tested machine torque; $l_{1,2}$ is respectively the active length of the backward-skewed and forward-skewed slices; $\psi_{d,q}$ is the dq-axis flux linkages. It is noted that the torque T_e is an nonvectorial value and therefore the same for both the skewed- and unskewed references.

$$\psi_{d1(0)} = \psi_{d1}\cos(\alpha) + \psi_{q1}\sin(\alpha) \tag{8}$$

$$\psi_{q1(0)} = -\psi_{d1}\sin(\alpha) + \psi_{q1}\cos(\alpha) \tag{9}$$

$$\psi_{d2(0)} = \psi_{d2}\cos(\alpha) - \psi_{q2}\sin(\alpha) \tag{10}$$

$$\psi_{q2(0)} = \psi_{d2}\sin(\alpha) + \psi_{q2}\cos(\alpha) \tag{11}$$

$$T_e(i_{d0}, i_{q0}) = \frac{l_1 T_{e1}(i_{d0}, i_{q0}) + l_2 T_{e2}(i_{d0}, i_{q0})}{l_1 + l_2} \tag{12}$$

$$\psi_d(i_{d0}, i_{q0}) = \frac{l_1 \psi_{d1(0)}(i_{d0}, i_{q0}) + l_2 \psi_{d2(0)}(i_{d0}, i_{q0})}{l_1 + l_2} \tag{13}$$

$$\psi_q(i_{d0}, i_{q0}) = \frac{l_1 \psi_{q1(0)}(i_{d0}, i_{q0}) + l_2 \psi_{q2(0)}(i_{d0}, i_{q0})}{l_1 + l_2} \tag{14}$$

B. Analysis of IPM Traction Machine with Skewed Rotor using Proposed Method

The stator flux linkage and torque maps of the tested machine without skewing are presented in Fig. 8. Based on the relation between dq-axis currents under the skewed reference and the unskewed reference in (1) to (4), the relevant stator flux linkage and torque maps with skewed rotor for the tested machine [see Figs. 1(b) and 1(c)] could be obtained as shown in Fig. 9. To demonstrate the effectiveness of the proposed method, the difference between the proposed method [see Fig. 9] and FEA result [see Fig. 6] is respectively presented in Fig. 10(a) and 10(b). As can be seen, under the proposed method, a maximum difference up to 0.2% over main dq-axis current operation region could be derived for both the stator flux linkage [see Fig. 10(a)] and the electromagnetic torque [see Fig. 10(b)].

Based on the obtained stator flux linkage and torque maps under the proposed method in Fig. 9, relevant dq-axis current reference LUTs for control development of the tested IPM machine could be generated [1] as shown in Fig. 11. In the next section, these current reference LUTs are employed to study the machine efficiency over torque-speed performance.

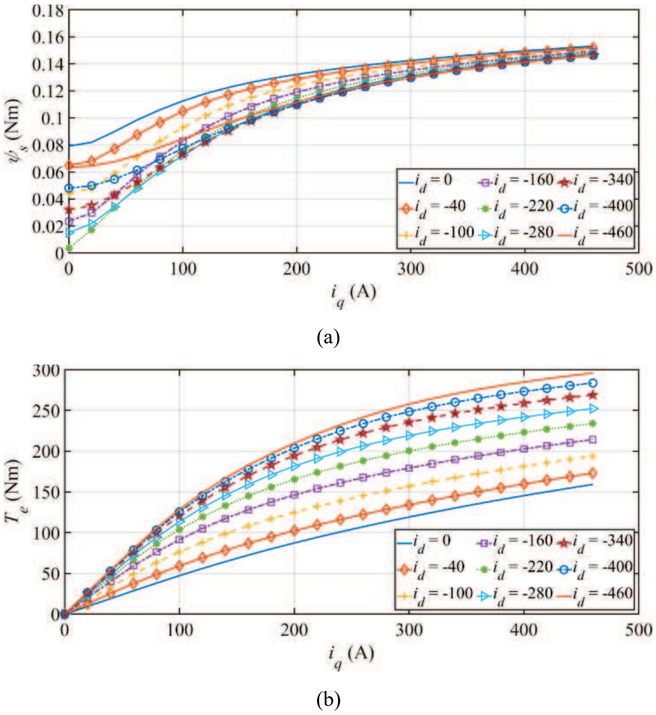

Fig. 8. Tested IPM machine characteristics with unskewed rotor, FEA model. (a) Stator flux linkage. (b) Torque.

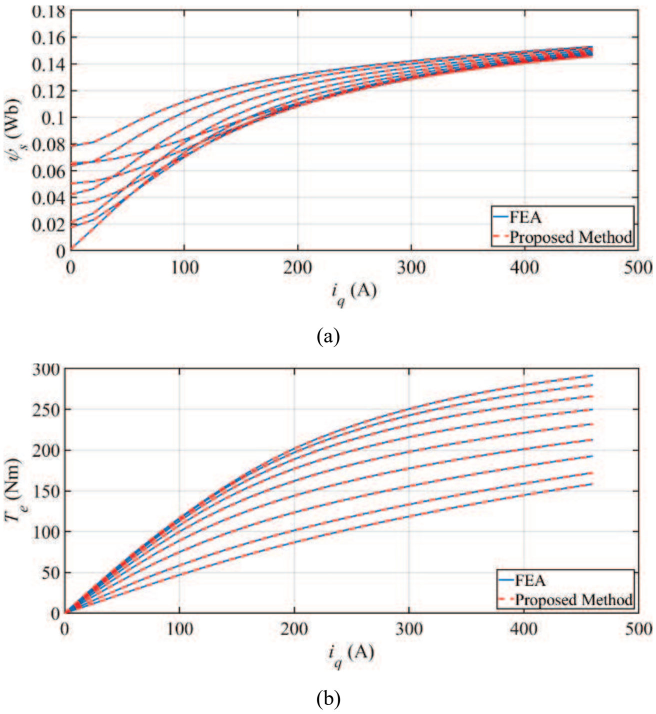

Fig. 9. Tested IPM machine characteristics with multi-slice rotor predicting from the unskewed model, proposed technique. (a) Stator flux linkage. (b) Torque.

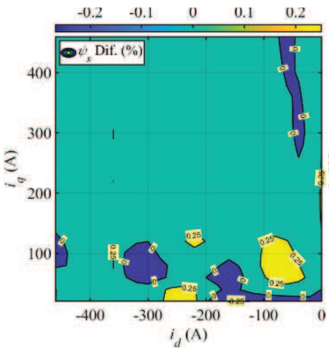

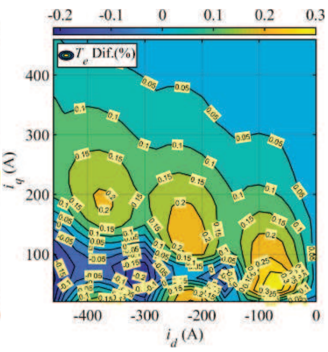

(a) (b)

Fig. 10. Difference between proposed method and FEA. (a) Stator flux linkage. (b) Torque.

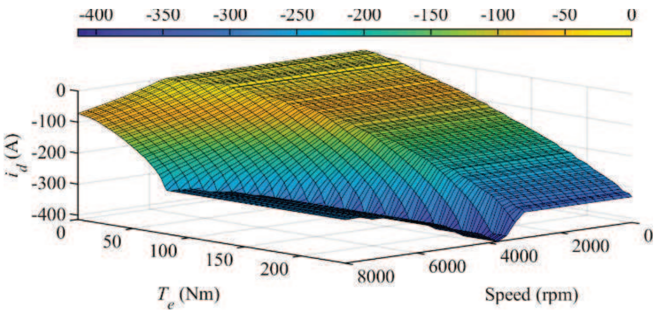

(a)

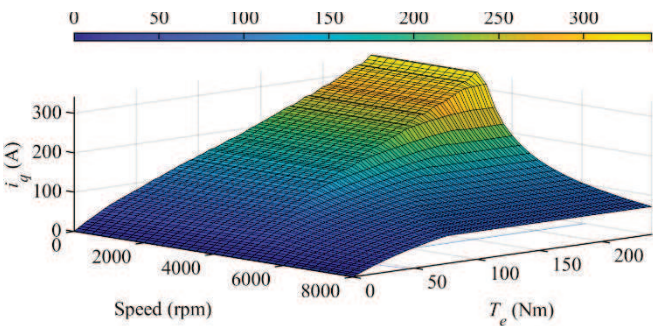

(b)

Fig. 11. *Dq*-axis current reference LUTs generated from stator flux linkage and torque maps under proposed method [see Fig. 9]. (a) *D*-axis current reference. (b) *Q*-axis current reference.

IV. Analysis and Experimental Results

In the section, analysis and experimental validation of the proposed method on model analysis and control development for the tested IPM machine with skewed rotor using the unskewed machine model is presented. The test-rig is shown in Fig. 12(a) where the dyno is controller under speed control mode and the tested IPM machine is controlled under torque control mode using *dq*-axis current reference LUTs obtained from the proposed technique [see Fig. 11]. A torque transducer (MAGTROL TM-313) is employed to sense the machine torque and active power. The machine efficiency is measured by a high-precision power analyzer (YOKOGAWA WT5000). Measured back-EMF of the tested machine is depicted in Fig. 12(b).

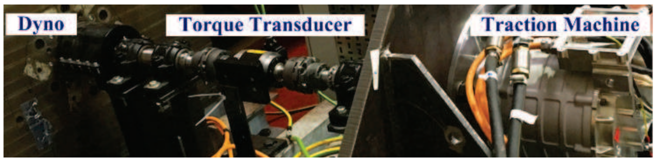

(a)

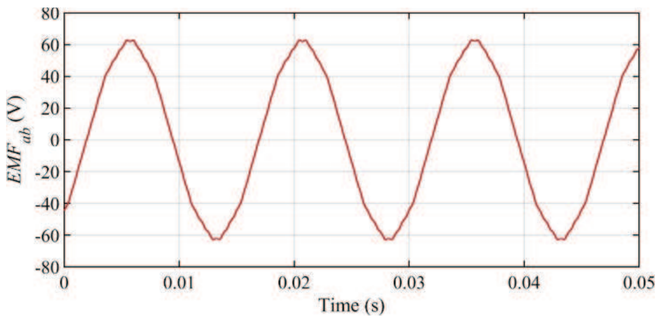

(b)

Fig. 12. Test-rig for proposed model validation. (a) Tested IPM machine. (b) Back-EMF at 1000rpm.

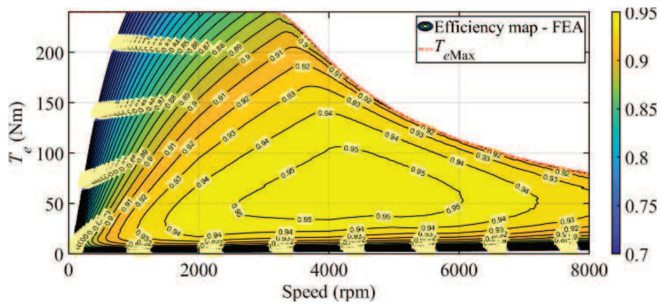

(a)

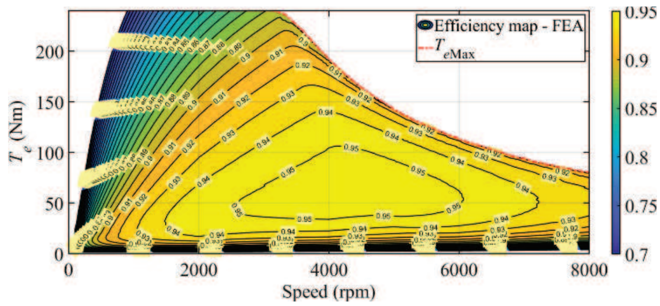

(b)

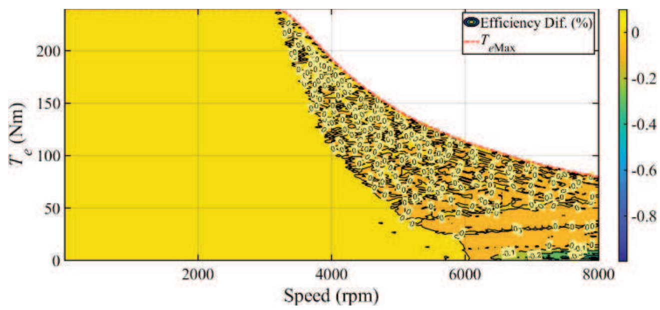

(c)

Fig. 13. Tested IPM machine efficiency maps. (a) Efficiency map with *dq*-axis current references generated from FEA model [see Fig. 6]. (b) Efficiency map with *dq*-axis current references generated from proposed method [see Fig. 9]. (c) Efficiency difference.

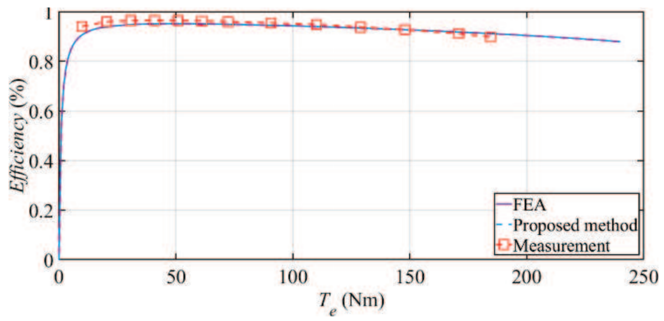

Fig. 14. Measured efficiency of tested IPM machine at 3000rpm under different demanded torques.

The efficiency map of the tested IPM machine under FEA-based model is presented in Fig. 13(a) and the relevant efficiency map of the tested machine using the obtained *dq*-axis current references under the proposed method [see Fig. 11] is depicted in Fig. 13(b). As can be seen, by employing the proposed method, a very similar efficiency as that with FEA could be achieved for the tested IPM machine. Therefore, for IPM machine with multi-skewed rotor slices, the proposed technique for obtaining skewed machine model from an unskewed model is highly essential due to not requiring extensive computational FEA for each rotor slice. For further demonstration, efficiency difference between the FEA and proposed method is illustrated in Fig. 13(c) where a maximum up to 0.2% efficiency could be observed for the proposed method over main torque-speed operation region.

The measurement of the tested machine efficiency is depicted in Fig. 14 where a good agreement between the predicted FEA and measured results could be observed. It is noted that the predicted efficiency is calculated based on a machine winding temperature assumption as 120 Celsius degrees. Therefore, under low demanded torque associated with low winding temperature, a higher measured efficiency than the predicted FEA could be achieved.

V. Conclusions

The paper presents a simplified analysis and control development method for IPM traction machines with skewed rotor using unskewing machine model. It has been shown that analysis model for an IPM machine with multi-slice skewed rotor could be obtained via the unskewed machine model using relevant modified *dq*-axis current associated with the skewed information without FEA requirement for each skewed slice. The proposed method is validated by FEA and measurement on a high-speed high-power (8000rpm, 80kW) IPM traction machine with multi-skewed rotor slices. It has been demonstrated that up to 0.2% stator flux linkage difference as well as 0.2% torque difference compared with FEA could be achieved for the skewed machine model derived from the proposed method. It has been presented that up to 0.1% efficiency difference compared with FEA could be achieved for the tested IPM machine using the obtained model.

Since the skewed effects are similar for synchronous machines, the proposed method is equally applicable to other synchronous machine types such as surface-mounted PM (SPM) machine, synchronous reluctance machine, and PM-assisted synchronous reluctance machine.

References

[1] K. D. Hoang, P. Lazari, K. Atallah, J. Birchall, and S. Calverley, “Evaluation of simplified model for control development of IPM traction machines,” in *IEEE Transactions on Transportation Electrification*, vol. 7, no. 2, pp. 779-792, June 2021.

[2] K. D. Hoang, "Simplified analytical model for rapid evaluation of interior PM traction machines considering magnetic nonlinearity," in *IEEE Open Journal of the Industrial Electronics Society*, vol. 1, pp. 340-354, 2020.

[3] X. B. Bomela and M. J. Kamper, "Effect of stator chording and rotor skewing on performance of reluctance synchronous machine," in *IEEE Transactions on Industry Applications*, vol. 38, no. 1, pp. 91-100, Jan.-Feb. 2002.

[4] R. Islam, I. Husain, A. Fardoun and K. McLaughlin, "Permanent-magnet synchronous motor magnet designs with skewing for torque ripple and cogging torque reduction," in *IEEE Transactions on Industry Applications*, vol. 45, no. 1, pp. 152-160, Jan.-feb. 2009.

[5] Y. S. Chen, Z. Q. Zhu and D. Howe, "Calculation of *d*- and *q*-axis inductances of PM brushless ac machines accounting for skew," in *IEEE Transactions on Magnetics*, vol. 41, no. 10, pp. 3940-3942, Oct. 2005.

[6] G. Qi, J. T. Chen, Z. Q. Zhu, D. Howe, L. B. Zhou and C. L. Gu, "Influence of skew and cross-coupling on flux-weakening performance of permanent-magnet brushless AC machines," in *IEEE Transactions on Magnetics*, vol. 45, no. 5, pp. 2110-2117, May 2009.

[7] P. Lazari, B. Sen, J. Wang and X. Chen, "Accurate *d-q* axis modelingof synchronous machines with skew accounting for saturation," in *IEEE Transactions on Magnetics*, vol. 50, no. 11, pp. 1-4, Nov. 2014.